THE JOURNAL OF PHYSICAL CHEMISTRY C

Article

pubs.acs.org/JPCC

Blinking, Flickering, and Correlation in Fluorescence of Single Colloidal CdSe Quantum Dots with Different Shells under Different Excitations

Li Li,[†] Guangjun Tian,[‡] Yi Luo,[‡] Hjalmar Brismar,[†] and Ying Fu*[,†]

[†]Department of Applied Physics, Royal Institute of Technology, SE-106 91 Stockholm, Sweden and Science for Life Laboratory, Karolinska Institutet, Science Park, SE-171 65, Solna, Sweden

[‡]Division of Theoretical Chemistry and Biology, School of Biotechnology, Royal Institute of Technology, SE-106 91 Stockholm, Sweden

ABSTRACT: We studied the fluorescence spectra from single CdSe core-CdS/ZnS and CdS/CdZnS/ZnS shell colloidal quantum dots (QDs) (different shell thicknesses and different surface ligands) under different optical excitations. It was found that the single QD blinks (on and off) at low excitation and flickers (without distinguishable on and off) under high excitation. Theoretical analysis suggests that under low excitation the single QD blinks due to transfer of the photogenerated electron and hole between QD core states and surface states, and the transfer rate is inversely proportional to the shell thickness, as demonstrated experimentally. Under high excitation, the photogenerated electron and hole via interband excitation are further excited via intraband excitation, which will keep the electron and hole from relaxing to the ground exciton state, therefore significantly suppressing the radiative interband recombination, resulting in QD flickering. It was further observed experimentally that the fluorescence events from two neighboring QDs under high excitation are correlated. The correlation can be most possibly understood that one QD, which is kept at the excited state by the high excitation, radiatively recombines under the stimulation of the emission from its neighboring QD.

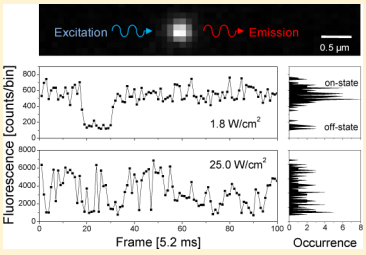

INTRODUCTION

During the last 30 years, semiconductor quantum dots (QDs) have been widely studied for various applications such as solar cells,[1,2] light-emitting diodes (LEDs),[3−5] QD lasers,[6−8] and QD photodetectors.[9,10] With superior optical properties of high brightness and photobleaching resistance, QDs have attracted further attention in the recent ten years as an alternative to traditional organic dyes for biomedical imaging[11−13] including single-particle tracking (SPT).[14,15] However, the fluorescence signal from single QDs is normally not steady. It displays irregular on (bright) and off (dark) cycles under continuous irradiation, known as fluorescence blinking or intermittency.[14−16] QD blinking can be a significant drawback in many applications such as information loss in SPT and reduced quantum yield.[4]

The mechanism of blinking has been intensely investigated, and several theories have been proposed. One theory involves Auger recombination where the strong interaction between multiple excitons leads to the ejection of an electron or a hole from the QD, resulting in a charged QD, in which the newly formed exciton will recombine via fast and nonradiative decay processes.[17−20] Another theory proposes that photoexcited hot carriers transfer to the QD surface and are captured by the trap states that induce the off state.[17,18,21−25] However, the detailed information about the mechanism of QD blinking is still unclear, and most possibly both processes are involved simultaneously.[21] Furthermore, it was reported recently that the energy transfer between neighboring QDs due to dipole−dipole interaction affects the QD blinking,[26−28] and the blinking behavior of QDs depends on excitation intensity.[20,21,25,29]

In this work, we attempt to shed more light on single QD fluorescence. Three types of CdSe-based QDs, with different shell thicknesses and different surface ligands, were investigated under different excitation powers. Theoretical analyses were also performed to understand experimental results.

EXPERIMENTAL DETAILS

QD Sample Preparation. Our QDs were chemically synthesized following common recipes; see, e.g., refs 30 and 31 and our early works.[2,32] The CdSe-CdS/CdZnS/ZnS QD, with an emission-peak wavelength of 601 nm ($\hbar\omega_{QD}$ = 2.06 eV), consists of a CdSe core with a diameter of 4.0 nm, a 2-monolayer (ML) CdS shell, a 4-ML CdZnS shell, and a 1.5-ML ZnS shell. The total diameter of this QD is 9.0 nm, and the shell thickness is 5.0 nm. The CdSe-CdS/ZnS QD, with an emission wavelength of 622 nm ($\hbar\omega_{QD}$ = 1.99 eV), consists of a CdSe core with a diameter of 4.6 nm, a 2-ML CdS shell, and a 1.5-ML ZnS shell. The total diameter of this QD is 6.9 nm, and the shell thickness is 2.3 nm.

Received: December 5, 2012
Revised: February 5, 2013
Published: February 7, 2013

The above two types of QDs are ODA-coated and oil-soluble. To study the effect of the surface ligands on the optical properties of the QDs, we also replaced ODA ligands on oil-soluble CdSe-CdS/CdZnS/ZnS QDs with 3-MPA so that the resulting QDs become water soluble.[32]

Standard structure characterizations of these QDs have been performed, and details were published; see, e.g., refs 2 and 32.

In short, we study three types of QDs, oil-soluble CdSe-CdS/CdZnS/ZnS and CdSe-CdS/ZnS QDs (surface ligand ODA) and water-soluble CdSe-CdS/CdZnS/ZnS QDs (surface ligand 3-MPA).

Single QD Fluorescence Imaging and Data Analysis. QD samples for fluorescence study were prepared by adding 5 μL of QD solutions (concentration 1 pM) on glass coverslips. After drying, the samples were transferred and mounted on the microscope. An AxioObserver.D1 microscope (Carl Zeiss) equipped with a mercury lamp (HBO 100, Carl Zeiss), a filter set (Exciter: FF02-435/40-25, Dichroic: FF510-Di02-25 × 36, Emitter: FF01-500/LP-25, Semrock), an EMCCD camera (Andor), and a 100 × 1.4 NA oil immersion objective (Carl Zeiss) were used to observe and record QD fluorescence which was analyzed by using ImageJ software.[33] In our fluorescence imaging system, QDs were excited by the light within the wavelength range 415−455 nm centered at 436 nm ($\hbar\omega_{ex}$ = 2.85 eV) from a mercury lamp. The illumination area was about 280 μm^2, as shown in Figure 1. By adjusting the aperture

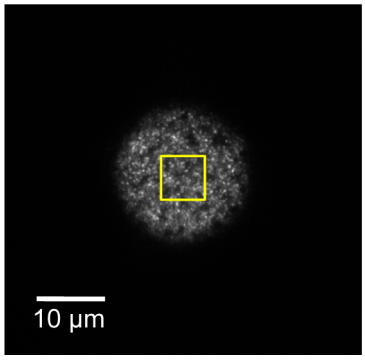

Figure 1. Illumination area. The yellow box represents the recording area (imaging frame) which is 64 × 64 pixels (6.4 × 6.4 μm^2).

diaphragm in the microscope and the mercury lamp control panel, we could tune the light power illuminated in this area. The four different optical powers used to excite QDs, which were measured by an optical power meter (Thorlabs), were 5, 11, 34, and 70 μW, corresponding to excitation power densities of 1.8, 3.9, 12.1, and 25.0 W/cm^2. The size of each imaging frame was 64 × 64 pixels (6.4 × 6.4 μm^2), as shown in Figure 1. The time duration of each image frame was 5.2 ms (exposure time 4.29 ms and readout time 0.91 ms).

Figure 2 shows the fluorescence distribution profile across a single QD. It is observed here that the diameter of the bright area from a single QD is about 1.0 μm, and the full width at half-maximum (fwhm) of the intensity distribution is about 0.3 μm which is comparable with the optical resolution of the microscope. Moreover, it was found in our experimental setup that these two values do not vary during the change of the excitation power.

The fluorescence signal $I(t)$ of each individual QD in each frame was measured as the maximal gray value in the analysis area of 4 × 4 pixels (0.4 × 0.4 μm^2), as shown in Figure 3.

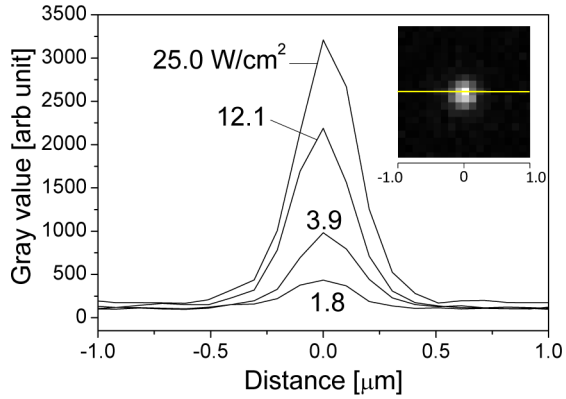

Figure 2. Fluorescence distribution profile across a single QD shown in the inset.

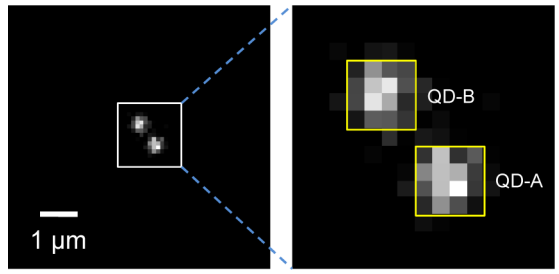

Figure 3. One typical image frame in which there are two oil-soluble CdSe-CdS/CdZnS/ZnS QDs, A and B, at a spatial distance of 0.66 μm from each other.

When two neighboring QDs are too close to each other such as the distance between them is shorter than 0.6 μm, the analysis area is reduced to 3 × 3 pixels (0.3 × 0.3 μm^2) or even 2 × 2 pixels (0.2 × 0.2 μm^2) to eliminate the crosstalk between two QD signals. Note that we also use the maximal gray value in the analysis area around the QD as the QD fluorescence signal to avoid possible problems related to the light diffusion.

To investigate the fluorescence of a single QD under the influence of a neighboring QD, a structured illumination microscope (Zeiss Elyra PS) equipped with a spectrometer and a 63 × 1.4 NA oil immersion objective (Carl Zeiss) was used to measure fluorescence images of QDs. Oil-soluble CdSe-CdS/CdZnS/ZnS QDs with the emission peak at 601 nm dispersed on the glass coverslip were excited by the laser line of 488 nm. The total scanning wavelength region was 562−646 nm with a resolution of 2.9 nm. The size of each imaging frame was 512 × 512 pixels (26.9 × 26.9 μm^2). The fluorescence intensity in each wavelength point was measured as the mean value in the area enclosed by the yellow line, as shown in Figure 13 (a), or around a single QD which is not shown because the area is so small.

RESULTS AND DISCUSSION

Single QD Blinking and Flickering. Typical fluorescence spectra $I(t)$ in the time domain are shown in Figure 4(a−d′) under four different optical excitations. Here we observe that at low excitations (1.8 and 3.9 W/cm^2) the fluorescences demonstrate clearly the on and off states, i.e., blinking. During the on state, $I(t)$ does not reduce to the background level, and during the off state, $I(t)$ stays close to the background level. At high excitation powers (12.1 and 25.0 W/cm^2) the fluorescence spectra are composed of short emission events such that $I(t)$

dx.doi.org/10.1021/jp311975h | J. Phys. Chem. C 2013, 117, 4844−4851

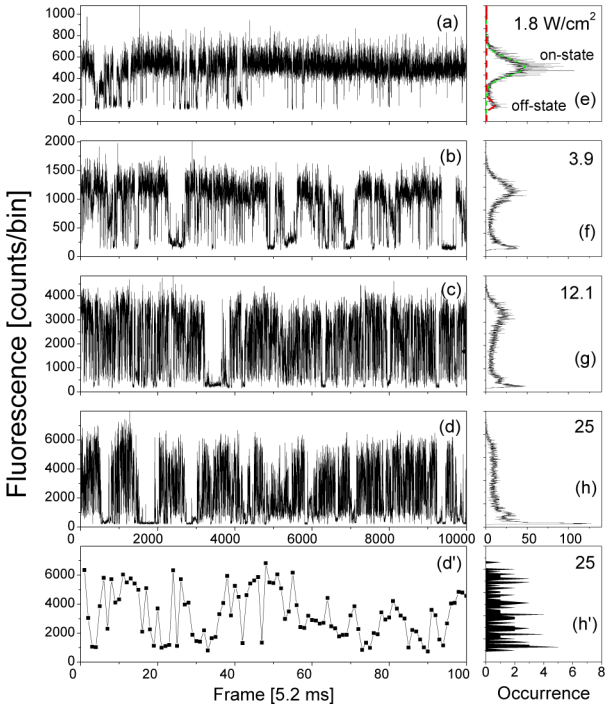

Figure 4. (a–d′) Fluorescence spectra of a single oil-soluble CdSe-CdS/CdZnS/ZnS QD under four different excitations. (e–h′) Occurrence of fluorescence intensity.

increases from the background level to a very high level and then reduces quickly to the background, which is normally referred to as flickering. Figure 4(d′) shows only the first 100 frames of the total 10 000 frames in Figure 4(d), demonstrating the flickering more clearly. The phenomena are more clearly reflected in the occurrence spectra of Figure 4(e–h′), which were obtained by counting the number of times that the QD fluoresces at a specific intensity.

We fitted the occurrence spectra by two Gaussian peaks, the green dashed on-state peak, and the red dashed off-state peak in Figure 4(e) and then calculated the on-state rate as the ratio between the on-state peak area and the total area of the occurrence spectrum. The results are presented in Figure 5 for the three types of QDs under investigation (50 randomly chosen QDs for each QD type, in total 150 QDs). The statistic

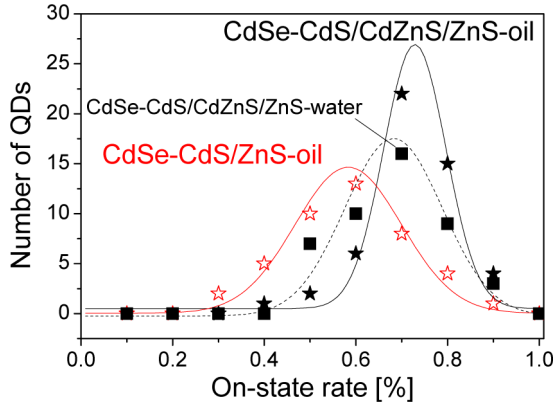

Figure 5. On-state ratios of the three types of QDs under investigation. Excitation power 1.8 W/cm^2. The lines are fitted Gaussian lines.

feature remains the same when only 60 QDs (20 for each QD type) are involved in the statistical analysis. The conclusion is clear: CdSe-CdS/CdZnS/ZnS, with a shell of 5.0 nm, stays at 73% at the on state, while the CdSe-CdS/ZnS QD, with a shell of 2.3 nm, stays at 58% at the on state. The result is not much affected by surface ligand exchange (from ODA to 3-MPA).

Figure 6 shows the energy band diagram of the QD from solid state theory,[2,4] the highest occupied molecular orbits

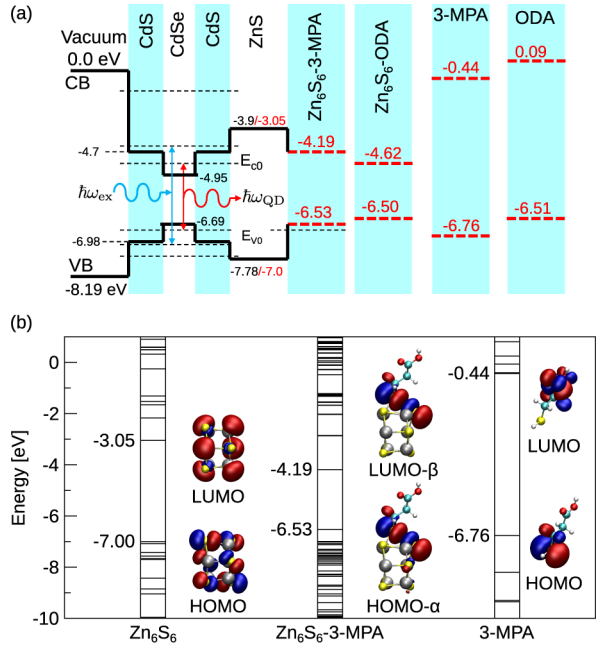

Figure 6. Conduction-band (CB) and valence-band (VB) structures of CdSe-CdS/ZnS QD, HOMO and LUMO levels (dashed lines) of surface ligands, Zn_6S_6–3-MPA, and Zn_6S_6–ODA molecules (a). Frontier HOMO and LUMO orbitals of Zn_6S_6–3-MPA are shown in (b).

(HOMOs), and the lowest unoccupied molecular orbits (LUMOs) of surface ligand 3-MPA and ODA, Zn_6S_6, and Zn_6S_6–3-MPA [Figure 6(b), energy diagram of Zn_6S_6–ODA is similar] obtained by density functional theory with the B3LYP exchange-correlation functional with a mixed basis set 6-31+g(d) (for nonmetal atoms) + LANL2DZ (for Zn atoms) by the Gaussian 09 program.[34] Frequency calculations were performed to ensure the absence of imaginary frequency modes.

It can be observed by Figure 6(a) and Figure 7(a) that when a photon $\hbar\omega_{ex}$ is absorbed by an electron initially occupying a VB state in the QD core the electron will transit from the VB state to an empty CB state, leaving the VB state unoccupied, i.e., creating a VB hole. The process is called interband excitation. At low excitation, i.e., low photon flux (microsecond average time interval between two successive photons, see below), the fluorescence of a single QD is basically continuous in the observation bin of milliseconds that as soon as there comes in a photon it will be absorbed to generate a photoexcited electron in the CB and a photoexcited hole in the VB. A photoexcited electron and hole will subsequently relax to the ground exciton state via many nonradiative relaxations, most predominantly resonant and nonresonant electron–phonon scatterings (single resonant electron–phonon scattering occurs on the picosecond time scale in a common colloidal CdSe-based QD; see, e.g., ref 35). The

dx.doi.org/10.1021/jp311975h | J. Phys. Chem. C 2013, 117, 4844–4851

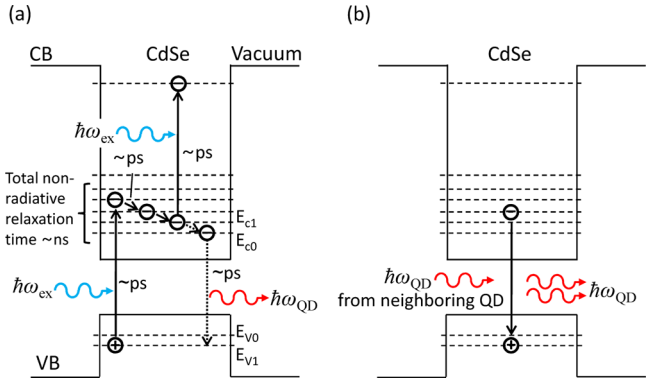

Figure 7. (a) Schematic diagram about the mechanism of QD flickering. (b) Time correlation of fluorescences from two neighboring QDs induced by stimulated emission.

ground exciton then radiatively recombines to emit a photon $\hbar\omega_{QD}$. The whole process, starting from the photogenerations of the CB electron and VB hole, to the many resonant and nonresonant nonradiative electron–phonon scatterings, to the exciton recombination, takes about 10 ns.[36]

We notice in Figure 6 discrepancies between the HOMO/LUMO levels of Zn_6S_6 and bulk ZnS due to the limited size of Zn_6S_6 that can be treated by first-principles theory and thus expect similar deviations between energy levels of real QD-ligand molecules and the simulated Zn_6S_6–3-MPA and Zn_6S_6–ODA molecules. Including such deviations, we still observe that the HOMO and LUMO levels of Zn_6S_6–3-MPA and Zn_6S_6–ODA molecules are very close to the ground states of the electron and hole in the QD core. The coupling between the electron and hole states in the QD core and the surface HOMO and LUMO will channel the photogenerated carriers from the QD core to the QD surface, thereafter separating the electron and hole from each other, thus prohibiting the radiative recombination between them until the electron and hole are all in the QD core. This most probably causes the observed on and off states in the single-QD fluorescence spectrum. This also agrees with our experimental data that a QD with a thicker shell stays longer at the on state (a thicker shell reduces transition of photogenerated carriers between QD core states and surface states); see also refs 23–25. The exchange of surface ligands from ODA to 3-MPA does not affect the statistic feature since the HOMO and LUMO levels of the two surface ligands are very similar.

In our early work[32] we did a first-principles study of the HOMO and LUMO of many common surface ligands including 3-MPA and ODA and found that the HOMOs are very close to the ground hole state in the QD core. The results were used by Xu et al. to understand observed shell thickness dependent hole transfer.[22] In our current work, we show by the first-principles study that not only the HOMOs of ligands (3-MPA and ODA) but also the HOMO-αs of conjugated QD-ligand molecules are close to the hole state in the QD core. This provides a very solid base for understanding QD-ligand experiments[32] and the hole transfer experiments of Xu et al.[22]

Figure 4 shows that at high excitation the single QD flickers in the time bin of milliseconds. As mentioned before, our excitation intensity W varies from 1.8, 3.9, 12.1, to 25.0 W/cm^2. We now try to estimate the number of photons that incident into a single QD and the absorption rate of the incident phonon by the QD. In our previous work,[37] we calculated the energy of the electromagnetic field that penetrates into the QD under a CW illumination, where the QD is described by a dielectric sphere including the exciton–polariton effect. It was found that for a CdSe-based QD with a fluorescence wavelength of 550 nm about 25% of the electromagnetic field with a wavelength of 436 nm can get into the QD, and the remaining 75% will be scattered. For the excitation wavelength of 436 nm ($\hbar\omega_{ex}$ = 2.85 eV), the number of photons n_{ex} that fall per second on a surface area S is

$$n_{ex} = 25\% \times \frac{WS}{\hbar\omega_{ex}} \tag{1}$$

When we consider the cross section of a single QD with a radius a of 5 nm, $S = \pi a^2$, the average time interval τ between two successive incident photons is 1289, 595, 192, and 92 ns, respectively. Thus, at high excitation (W = 12.1 and 25.0 W/cm^2), τ is close to the electron–hole nonradiative relaxation time from the high-energy exciton state to the ground exciton state, indicating that the sequential cycle (period of 10 ns, see ref 36) of excitation–relaxation–recombination at high excitation will be strongly perturbed, and new processes will emerge.

Since biexciton quantum yield was shown to be rather low,[38] and our optical excitation powers are relatively low (in the work of Peterson and Nesbitt, the optical powers were 66, 120, and 230 W/cm^2[20]), we focus on the single exciton. We denote the envelope wave function of an electron state in the QD as ψ_i and its energy E_i. Interband optical transition between one CB state and one VB state is described by its optical transition matrix element[39]

$$P_{inter} = \langle \psi_j u_c | \mathbf{p} | \psi_i u_v \rangle = \mathbf{p}_{cv} \langle \psi_j | \psi_i \rangle \approx \mathbf{p}_{cv} \tag{2}$$

where $\mathbf{p}$ is the electron momentum; u_c and u_v are CB and VB Bloch functions; and $\mathbf{p}_{cv} = \langle u_c | \mathbf{p} | u_v \rangle$ is the optical matrix element between the CB and VB. Between two states within the same band, either CB or VB, referred to as intraband transition, the optical matrix element is

$$\begin{aligned} P_{intra} &= \langle \psi_j u_c | \mathbf{p} | \psi_i u_c \rangle = \langle \psi_j | \mathbf{p} | \psi_i \rangle = m_0 \left\langle \psi_j \left| \frac{d\mathbf{r}}{dt} \right| \psi_i \right\rangle \\ &= \frac{im_0}{\hbar} \langle \psi_j | [H_0, \mathbf{r}] | \psi_i \rangle = \frac{im_0(E_j - E_i)}{\hbar} \langle \psi_j | \mathbf{r} | \psi_i \rangle \\ &\approx \frac{im_0(E_j - E_i)}{\hbar} a \end{aligned} \tag{3}$$

where m_0 is the electron mass and a is the QD radius.

We now estimate quantitatively these two transition rates. For common semiconductors $E_p = p_{cv}^2/2m_0$ = 20 eV[40] so that the interband transition matrix element $P_{inter} = p_{cv}$ = 2.4 × 10^{-24} kg·m/s. For QDs with a radius of 5 nm, P_{intra} = 19.8 × 10^{-24} kg·m/s when $E_j - E_i = \hbar\omega_{ex}$ = 2.85 eV. In other words, the intraband transition rate is quite large, even larger than the interband transition. Note that the intraband transition will be even stronger when the high densities of high-energy electron and hole states are taken into account. Thus, at high excitations, the photogenerated electron and hole via interband excitation will be further excited via intraband excitation and fluctuate between the vibrational levels in the excited states, which prevents the electron and hole from relaxing to the ground exciton state for radiative recombination, thereafter leading to the flickering, as shown in Figure 7(a).

dx.doi.org/10.1021/jp311975h | J. Phys. Chem. C 2013, 117, 4844–4851

The reduced radiative recombination is reflected in its relationship with the excitation power, as shown in Figure 8,

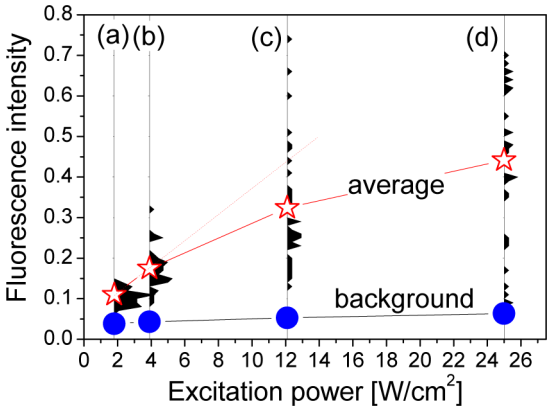

Figure 8. Average QD fluorescence (stars) and background (circles) vs excitation power. The four vertical spectra show the number of QDs at the specific fluorescence intensity. 35 oil-soluble CdSe-CdS/CdZnS/ZnS QDs were involved. The peak number of QDs in (a) is 9.

which is obtained by averaging over 10 000 frames. Thirty-finve oil-soluble CdSe-CdS/CdZnS/ZnS QDs were included, and the same 35 QDs were analyzed under the four different excitations. Another important aspect of the reduced radiative recombination is reflected in the statistic spectra (a–d) in Figure 8 that at high excitations QD fluorescence intensity distributes widely. Similar effects were found in the other two QD types under investigation. Note that the high excitation only intensifies and broadens the QD fluorescence peak (see ref 41).

The evolution from blinking to flickering was reported by Galland et al. in an electrochemical study,[18] while it was reported that the single QD fluorescence can be reversibly quenched by modifying an external electrochemical potential.[42] These two experiments can be well understood by the energy band diagrams of Figure 6 that the application of either a positive or a negative electrochemical potential modifies the couplings of the electron and hole states in the QD core and the surface states, resulting in the observed changes in the QD fluorescence.

Correlation of Fluorescences from Neighboring QDs. Furthermore, we have observed a correlation phenomenon between the flickering events of two neighboring single QDs. Figure 9 shows the fluorescence spectra of QD A and B in Figure 3 and their cross correlation which is quantified as[16]

$$g_{AB}(\tau) = \frac{\langle [I_A(t) - \bar{N}][I_B(t+\tau) - \bar{N}]\rangle_t}{\langle I_A(t) - \bar{N}\rangle_t \langle I_B(t+\tau) - \bar{N}\rangle_t} \quad (4)$$

where τ is the time interval and $\langle ... \rangle_t$ denotes the time average. $\bar{N}$ is the mean value of background signal $N(t)$ which is recorded at a nearby dark point. Note that $\bar{N}$ = 185 and 225, respectively, under the two excitations of 12.1 and 25.0 W/cm^2. Figure 9(c,d) indicates that under high excitations $g_{AB}(\tau)$ shows a peak at τ = 0, suggesting that the fluorescence events from the two QDs become correlated; i.e., the two QDs fluoresce synchronously, and the cross correlation is enhanced by increasing the excitation power.

Since the diameter of the bright area from the fluorescence of a single QD is about 1.0 μm (see Figure 2), light interdiffusions between the fluorescence signals of two neighboring QDs are

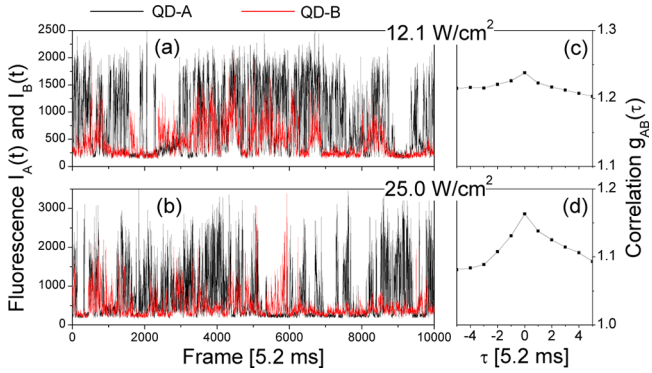

Figure 9. (a,b) Fluorescence spectra of two neighboring oil-soluble CdSe-CdS/CdZnS/ZnS QDs under high excitations. (c,d) Correlation between the fluorescence spectra in (a,b).

inevitable if the distance between the two QDs is below 1.0 μm. Assume that there is a diffusion of the fluorescence from QD B to QD A, so that the measured fluorescence signal from QD A becomes $I_A(t) + \alpha I_B(t)$. The cross correlation between $I_A(t) + \alpha I_B(t)$ and $I_B(t)$ is now

$$g'_{AB}(\tau) = \frac{\langle [I_A(t) + \alpha I_B(t) - \bar{N}][I_B(t+\tau) - \bar{N}]\rangle_t}{\langle I_A(t) + \alpha I_B(t) - \bar{N}\rangle_t \langle I_B(t+\tau) - \bar{N}\rangle_t} \quad (5)$$

By straightforward mathematical derivations, it is obtained that

$$g'_{AB}(\tau) = (1 - \alpha\beta) g_{AB}(\tau) + \alpha D g_{BB}(\tau) + \alpha C \quad (6)$$

where

$$\beta = \frac{\langle I_B(t)\rangle_t}{\langle I_A(t) - \bar{N}\rangle_t}, \; D = \frac{\langle I_B(t) - \bar{N}\rangle_t}{\langle I_A(t) - \bar{N}\rangle_t}, \; C = \frac{\bar{N}}{\langle I_A(t) - \bar{N}\rangle_t} \quad (7)$$

which are τ independent. Note that C is α-independent so will be neglected in the following discussion.

Figure 9(a, b) shows that $I_A(t)$ and $I_B(t)$ are comparable with each other and are well above $\bar{N}$, and β and D are in the order of 1. Thus, the effect of the light diffusion rests mainly on the value of α.

For the QD pair with a spatial distance of 0.66 μm in Figure 3, the fluorescence distribution profile is shown in Figure 10. Within the areas of 0.4 × 0.4 μm^2 from where the fluorescence

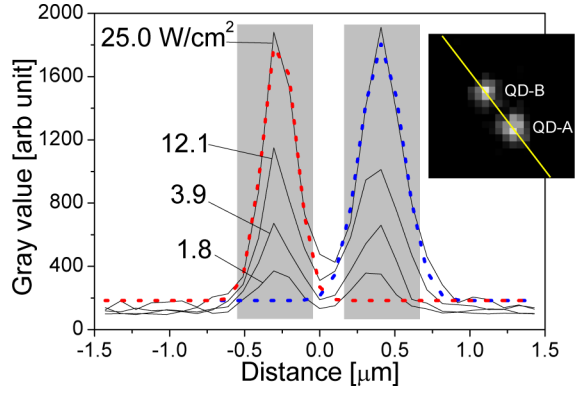

Figure 10. Fluorescence distribution profiles of QD A and B in Figure 3 along the yellow line in the inset. The blue and red dot curves are the fitted curves of QD A and B. Maximal gray values in gray areas were extracted as the fluorescence signals.

dx.doi.org/10.1021/jp311975h | J. Phys. Chem. C 2013, 117, 4844–4851

signals are obtained, there is basically no light interdiffusion, so α is negligibly small. Thus, $g'_{AB}(\tau) = g_{AB}(\tau)$ by eq 6, and the observed time-correlation effects remain.

To quantitatively characterize the correlation effect, we have studied many QD pairs by calculating the mean value

$$\bar{g}_{AB} = \frac{1}{10}\sum_{\tau} g_{AB}(\tau) \quad (8)$$

for $\tau = \pm1, \pm2, ..., \pm5$ and their standard deviation σ, then comparing $g_{AB}(0)$ with $\bar{g}_{AB} + \sigma$. The fluorescences are defined as correlated when $g_{AB}(0) > \bar{g}_{AB} + \sigma$. Furthermore, the correlation effect is defined more restrictively by $g_{AB}(0) > \bar{g}_{AB} + 2\sigma$. Figure 11 shows the statistic result of oil-soluble CdSe-CdS/CdZnS/ZnS QDs. It indicates that the time-correlation effect exists between two QDs when the distance between them is up to 1.2 μm.

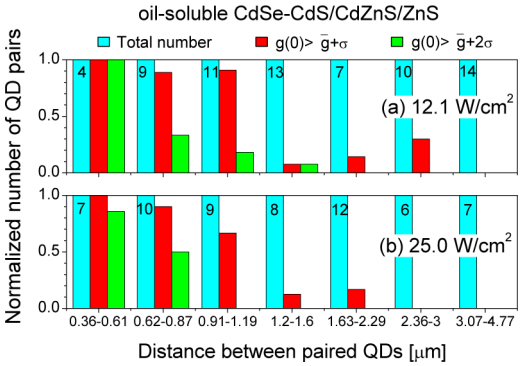

Figure 11. Statistic result of cross correlation analysis from paired oil-soluble CdSe-CdS/CdZnS/ZnS QDs with different spatial distances under different excitations. The values in the bar of total number indicate the numbers of QD pairs that are studied.

A similar correlation effect has been observed in water-soluble CdSe-CdS/CdZnS/ZnS QDs as well as oil-soluble CdSe-CdS/ZnS QDs (see Figure 12).

Note that the correlation effect is only observed under high optical excitation when QDs flicker, which is 12.1 and 25.0 W/cm^2 for our QDs. In other words, the correlation effect is strongly related with the flickering phenomenon.

As mentioned in the Introduction, Singh et al. recently showed that dipole−dipole interaction between two neighboring QDs can induce strong interference between the photoluminescence signals of the two QDs.[27] By adopting the energy transfer rate equation of Singh et al., it is easy to show that the dipole−dipole interaction between our paired QDs is negligible since the spatial separation between the two QDs under investigation is about 1 μm, much larger than the Forster radius (about 20 nm[27]).

Figure 13 shows the fluorescence spectra of two QD samples: one is densely packed (see Figure 13(a)), and the other is very diluted and dispersed and thus is basically composed of single QDs (see Figure 13(b)). A blue shift was observed in the emission peak of densely packed QDs in comparison with those of single QDs.

It is known by quantum mechanics of light−matter interaction (see, e.g., ref 43) that the radiative recombination of the electron−hole pair in the exciton state to the ground state occurs strongly when the energy of the photon is equal to the shifted energy (blue shift) of the exciton state. The energy shift is proportional to $N + 1$, where N is the number of

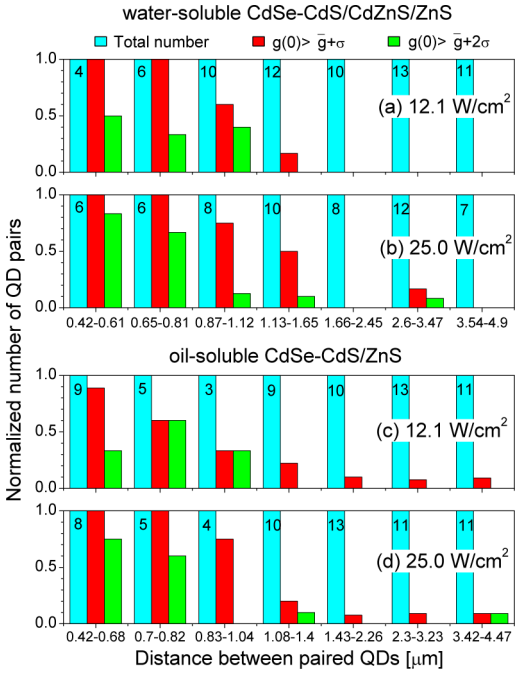

Figure 12. Same as Figure 11 but for water-soluble CdSe-CdS/CdZnS/ZnS QDs (a,b) and oil-soluble CdSe-CdS/ZnS QDs (c,d).

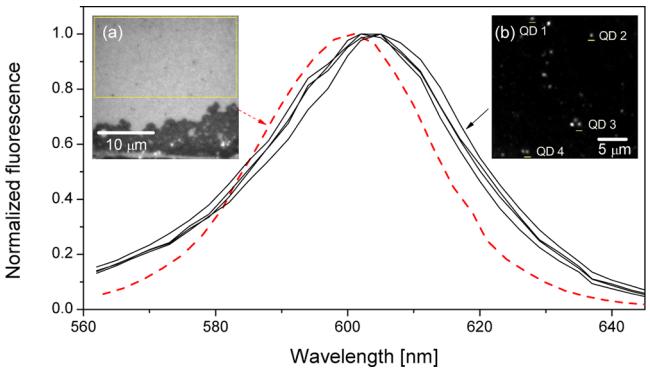

Figure 13. Effect of QD density on the fluorescence spectrum of QDs. The red dashed curve indicates the fluorescence spectrum of the densely packed QDs in the area enclosed by the yellow line shown in image (a). The four black curves represent the fluorescence spectra of four single QDs, QD1−4 shown in image (b), respectively.

photons before the radiative recombination process. We may therefore interpret the blue shift observed in Figure 13 in terms of stimulated emission that the fluorescence of well-separated QDs is dominated by spontaneous emissions ($N = 0$) of individual QDs, while the fluorescence of densely packed QDs is dominated by stimulated emissions ($N = 1$) of QDs under the influence of emissions from neighboring QDs. On the basis of this physical understanding, it can be believed that the most reasonable mechanism of the observed correlation under high excitation is the stimulated emission of QD A under the influence of the radiative emission from the neighboring QD B (see Figure 7(b)). QD A will experience a strong electromagnetic field of the emitted photon from QD B when QD A and B are close with each other. Moreover, the flickering phenomenon shows that the basic requirements of stimulated emission are fulfilled in that the fluorescence energy of QD B condenses into a strong pulse, while QD A is kept at the excited state. We also notice the difference between Figures 11 and 12,

dx.doi.org/10.1021/jp311975h | J. Phys. Chem. C 2013, 117, 4844−4851

that CdSe-CdS/CdZnS/ZnS QDs have a larger correlation effect area (distance between two neighboring QDs < 1.2 μm) than CdSe-CdS/ZnS QDs (distance between two neighboring QDs < 1 μm). This is expected because CdSe-CdS/CdZnS/ZnS QDs are brighter than CdSe-CdS/ZnS QDs, and the probability of stimulated emission between CdSe-CdS/CdZnS/ZnS QDs is higher than CdSe-CdS/ZnS QDs.

SUMMARY

We have observed the evolution of fluorescence blinking to flickering from single QDs when the excitation power was increased. Theoretical analysis shows that at low excitations the photogenerated electron and hole in the QD core transfer between the QD core states and QD surface states, resulting in QD blinking. This transfer process depends on the shell thickness, so that the QD blinking can be suppressed by a thick shell. Moreover, theoretical calculation shows that the intraband excitation rates of electron and hole are rather high so that under high excitation the interband-photoexcited electron and hole can easily be further excited via intraband excitation, which prevents the electron and hole from relaxing to the ground exciton state for radiative recombination, resulting in QD flickering. We have further observed experimentally that the fluorescence events from two neighboring QDs under high excitation are correlated. The time-correlation effect can be understood by the stimulated emission of one QD under the radiative emission from the neighboring QD.

AUTHOR INFORMATION

Corresponding Author

*E-mail: fu@kth.se.

Notes

The authors declare no competing financial interest.

ACKNOWLEDGMENTS

The work was supported by the Swedish Research Council (V.R.) and the Swedish National Infrastructure for Computing. We thank Dr. Otto Manneberg from Science for Life Laboratory, Sweden, for the help with the structured illumination microscope manipulation.

REFERENCES

(1) Kamat, P. V. *J. Phys. Chem. C* **2008**, *112*, 18737−18753.
(2) Ning, Z.; Tian, H.; Qin, H.; Zhang, Q.; Ågren, H.; Sun, L.; Fu, Y. *J. Phys. Chem. C* **2010**, *114*, 15184−15189.
(3) Anikeeva, P. O.; Madigan, C. F.; Halpert, J. E.; Bawendi, M. G.; Bulović, V. *Phys. Rev. B* **2008**, *78*, 085434.
(4) García-Santamaría, F.; Chen, Y.; Vela, J.; Schaller, R. D.; Hollingsworth, J. A.; Klimov, V. I. *Nano Lett.* **2009**, *9*, 3482−3488.
(5) Jang, E.; Jun, S.; Jang, H.; Lim, J.; Kim, B.; Kim, Y. *Adv. Mater.* **2010**, *22*, 3076−3080.
(6) Klimov, V. I.; Mikhailovsky, A. A.; Xu, S.; Malko, A.; Hollingsworth, J. A.; Leatherdale, C. A.; Eisler, H.-J.; Bawendi, M. G. *Science* **2000**, *290*, 314−317.
(7) Coleman, J.; Young, J.; Garg, A. *J. Lightwave Technol.* **2011**, *29*, 499−510.
(8) Grundmann, M.; Ledentsov, N.; Kirstaedter, N.; Heinrichsdorff, F.; Krost, A.; Bimberg, D.; Kosogov, A.; Ruvimov, S.; Werner, P.; Ustinov, V.; Kop'ev, P.; Alferov, Z. *Thin Solid Films* **1998**, *318*, 83−87.
(9) Höglund, L.; Holtz, P. O.; Ouattara, L.; Asplund, C.; Wang, Q.; Almqvist, S.; Petrini, E.; Malm, H.; Borglind, J.; Smuk, S.; Mikkelsen, A.; Lundgren, E.; Pettersson, H.; Andersson, J. Y. *Proc. SPIE* **2006**, *6401*, 640109−640121.
(10) Hellström, S.; Chen, Z.-H.; Fu, Y.; Qiu, M.; Soltanmoradi, R.; Wang, Q.; Andersson, J. Y. *Appl. Phys. Lett.* **2010**, *96*, 231110−231112.
(11) Medintz, I. L.; Tetsuo Uyeda, H.; Goldman, E. R.; Mattoussi, H. *Nat. Mater.* **2005**, *4*, 435−446.
(12) Resch-Genger, U.; Grabolle, M.; Cavaliere-Jaricot, S.; Nitschke, R.; Nann, T. *Nat. Methods* **2008**, *5*, 763−775.
(13) M. Molnár, M.; Friberg, P.; Fu, Y.; Brisslert, M.; Adams, M.; Chen, Y. *Cell Med. Part B: Cell Transplant.* **2010**, *1*, 105−112.
(14) Michalet, X.; Pinaud, F. F.; Bentolila, L. A.; Tsay, J. M.; Doose, S.; Li, J. J.; Sundaresan, G.; Wu, A. M.; Gambhir, S. S.; Weiss, S. *Science* **2005**, *307*, 538−544.
(15) Pinaud, F.; Clarke, S.; Sittner, A.; Dahan, M. *Nat. Methods* **2010**, *7*, 275−285.
(16) Qin, H.-Y.; Shang, X.-J.; Ning, Z.-J.; Fu, T.; Niu, Z.-C.; Brismar, H.; Ågren, H.; Fu, Y. *J. Phys. Chem. C* **2012**, *116*, 12786−12790.
(17) Krauss, T. D.; Peterson, J. J. *Nat. Mater.* **2012**, *11*, 14−16.
(18) Galland, C.; Ghosh, Y.; Steinbrueck, A.; Sykora, M.; Hollingsworth, J. A.; Klimov, V. I.; Htoon, H. *Nature* **2011**, *479*, 203−207.
(19) Wang, X.; Ren, X.; Kahen, K.; Hahn, M. A.; Rajeswaran, M.; Maccagnano-Zacher, S.; Silcox, J.; Cragg, G. E.; Efros, A. L.; Krauss, T. D. *Nature* **2009**, *459*, 686−689.
(20) Peterson, J. J.; Nesbitt, D. J. *Nano Lett.* **2009**, *9*, 338−345.
(21) Rosen, S.; Schwartz, O.; Oron, D. *Phys. Rev. Lett.* **2010**, *104*, 157404−157407.
(22) Xu, Z.; Hine, C. R.; Maye, M. M.; Meng, Q.; Cotlet, M. *ACS Nano* **2012**, *6*, 4984−4992.
(23) Qin, W.; Guyot-Sionnest, P. *ACS Nano* **2012**, *6*, 9125−9132.
(24) Vela, J.; Htoon, H.; Chen, Y.; Park, Y.-S.; Ghosh, Y.; Goodwin, P. M.; Werner, J. H.; Wells, N. P.; Casson, J. L.; Hollingsworth, J. A. *J. Biophotonics* **2010**, *3*, 706−717.
(25) Malko, A. V.; Park, Y.-S.; Sampat, S.; Galland, C.; Vela, J.; Chen, Y.; Hollingsworth, J. A.; Klimov, V. I.; Htoon, H. *Nano Lett.* **2011**, *11*, 5213−5218.
(26) Singh, M. R.; Schindel, D. G.; Hatef, A. *Appl. Phys. Lett.* **2011**, *99*, 181106.
(27) Singh, M. R.; Racknor, C.; Schindel, D. *Appl. Phys. Lett.* **2012**, *101*, 051115.
(28) Cox, J. D.; Singh, M. R.; Gumbs, G.; Anton, M. A.; Carreno, F. *Phys. Rev. B* **2012**, *86*, 125452.
(29) Bruhn, B.; Valenta, J.; Sangghaleh, F.; Linnros, J. *Nano Lett.* **2011**, *11*, 5574−5580.
(30) Li, J. J.; Wang, Y. A.; Guo, W.; Keay, J. C.; Mishima, T. D.; Johnson, M. B.; Peng, X. *J. Am. Chem. Soc.* **2003**, *125*, 12567−12575.
(31) Xie, R.; Kolb, U.; Li, J.; Basché, T.; Mews, A. *J. Am. Chem. Soc.* **2005**, *127*, 7480−7488.
(32) Ning, Z.; Molnár, M.; Chen, Y.; Friberg, P.; Gan, L.; Ågren, H.; Fu, Y. *Phys. Chem. Chem. Phys.* **2011**, *13*, 5848−5854.
(33) Abramoff, M. D.; Magelhaes, P. J.; Ram, S. J. *Biophotonics Int.* **2004**, *11*, 36−42.
(34) Frisch, M. J.; Trucks, G. W.; Schlegel, H. B.; Scuseria, G. E.; Robb, M. A.; Cheeseman, J. R.; Scalmani, G.; Barone, V.; Mennucci, B.; Petersson, G. A. et al. *Gaussian 09*, revision A. 02; Gaussian Inc.: Wallingford CT, 2009.
(35) Pandey, A.; Guyot-Sionnest, P. *Science* **2008**, *322*, 929−932.
(36) Fu, Y.; Ågren, H.; Kowalewski, J. M.; Brismar, H.; Wu, J.; Yue, Y.; Dai, N.; Thylén, L. *Europhys. Lett.* **2009**, *86*, 37003.
(37) Chen, Z.-H.; Hellström, S.; Ning, Z.-J.; Yu, Z.-Y.; Fu, Y. *J. Phys. Chem. C* **2011**, *115*, 5286−5293.
(38) Nair, G.; Zhao, J.; Bawendi, M. G. *Nano Lett.* **2011**, *11*, 1136−1140.
(39) Ridley, B. K. *Quantum Processes in Semiconductors*; Clarendon: Oxford, 1988; Chapter 5 Radiative Transitions, p 184.
(40) Lawaetz, P. *Phys. Rev. B* **1971**, *4*, 3460−3467.
(41) Molnár, M.; Fu, Y.; Friberg, P.; Chen, Y. *J. Nanobiotechnol.* **2010**, *8*, 2.
(42) Jha, P. P.; Guyot-Sionnest, P. *J. Phys. Chem. C* **2010**, *114*, 21138−21141.

(43) Gasiorowicz, S. *Quantum Physics*, 2nd ed.; John Wiley & Sons: New York, 1996; pp 453−459.